

*date:* March 13, 2003  
Original Dec 15, 00; Revised Jan 11, 01, PRS; Revised Mar 13, 03, DAL.

*to:* Distribution

*from:* P.R. Schunk, 9114, MS0826, Amy Sun (formerly 9114), S.Y. Tam (Imation Corp.) and K.S. Chen

*subject:* Elastoviscoplastic (EVP) Constitutive Model in GOMA: Theory, Testing, and Tutorial (GT- 019.3)

Elastoviscoplasticity, EVP, Solid Constitutive Equation, drying, residual stress, drying validation

*keywords:* Plasticity Equation, Plastic Viscosity, EVP Yield Stress, Stress Free Solvent Vol Frac, Mesh Stress Tensor, Viscoplastic Def\_Grad Tensor

*input records:*

## **Introduction**

This memo serves as a tutorial on the theoretical background and proper usage of the solid- material elastoviscoplastic constitutive model in GOMA. This work began with Ken Chen, 9114, and Siu-Yue Tam (formerly U. of New Mexico and now Imation Corporation) in 1997. After a year or so of theoretical development and GOMA implementation the model was ready for testing. Amy Sun, formerly 9114 and now of Intel Corp, was responsible for testing and evaluation on real-world solvent-polymer drying processes. Her findings led to several improvements, including a fully analytic Jacobian. This memo presents the final milestones of the project, and outlines some future research areas.

The elasto-viscoplastic constitutive model is usually thought of as an extension of the elastic constitutive model. Elastic models break down when material starts to fail (by bond breakage, local cavitation, etc.); elasto-viscoplastic constitutive models can be invoked to further predict the stress during elastic-viscoplastic flow. High stress is commonly found in drying coatings, not only around non uniformities and onset of defects, but towards the end of the drying process. Highly concentrated stress calls for a realistic viscoplastic model to account for material failure. While this is true, the elasto-viscoplastic model can do much more. It allows one to study material behavior beyond the elastic limit. With cyclic loading, energy dissipation can be calculated from the hysteresis loop. It can also allow one to study viscous flow when the yield stress is set to very low, albeit in a Lagrangian fashion and hence with a mesh-based finite element approach is quite limiting. A high priority for future development is for the integration of this model with the TALE algorithm (GT-005.3).

In this memo we outline some theoretical concepts underpinning the model in GOMA, present some usage tips in a tutorial fashion, and show results from three test problems (drying in one

dimension, drying in two dimensions, and simple tenting/stretching). The tutorial concludes with some trouble shooting and other usage tips as well.

## **Theoretical Developments**

### Model: Governing Equations and Boundary Conditions for the CRMPC Drying Problem and Other Generic Uses

The momentum balance (viz. static equilibrium equation referred to the current configuration) is:

$$\nabla \cdot \underset{\sim}{T}_s + \rho \underset{\sim}{g} = 0 \quad (\text{EQ 1})$$

where  $\underset{\sim}{T}_s$  is the Cauchy (true) stress. In general, and especially in drying processes, we consider only quasistatic deformation, viz. the inertia term is negligible and is thus absent in the momentum balance equation. (As an aside, it should be noted that the effect of inertia from advection of the stress free state can be handled in GOMA, even in this case if needed; see GT-005.3 and the **Convective Lagrangian Velocity** record in the user's manual SAND97-2404). In many problems, the effect of the weight of the material is small as well, as it is on any internal mass transfer processes, hence the gravitational force can usually be neglected. For coating materials that are significantly softer than the substrate on which it is coated, the substrate can be considered rigid. In most problems we specify no-slip of the material at a fixed boundary, viz. the components of the displacement vector  $\underset{\sim}{d}$  are taken as zero at rigid, stationary boundaries:

$$\underset{\sim}{d} = 0 \quad (\text{EQ 2})$$

A more natural condition of continuous displacement is automatically satisfied without specification for no-slip at interfaces between two materials, both of which are undergoing deformation and both of which are in the model:

$$\underset{\sim}{d}_{\text{material1}} = \underset{\sim}{d}_{\text{material2}} \quad (\text{EQ 3})$$

At free surfaces at which no external forces are applied, we desire the traction free boundary condition:

$$\underset{\sim}{n} \cdot \underset{\sim}{T}_s = 0 \quad (\text{EQ 4})$$

$\underset{\sim}{n}$  is the normal vector at the deformed free surface. Other traction boundary conditions supported in GOMA include those which allow a surface stress to be applied or some interaction with a fluid-stress from a neighboring material. Please see the GOMA Users's manual (SAND97-2404) for other options.

Distributio

Kinematics (Lagrangian Case)

A total Lagrangian description of the deformation is adopted and the deformation gradient  $\mathbf{F}$  is given by:

$$\mathbf{F} \equiv \frac{\partial \mathbf{x}}{\partial \mathbf{X}} \tag{EQ 5}$$

where this operator is really the gradient operator in the original (natural) configuration  $\mathbf{X}$  and  $\mathbf{x}$  is the vector representing current position of the material points. Vector  $\mathbf{x}$

$\mathbf{x}$  is the sum of the original position vector  $\mathbf{X}$  and the displacement vector  $\mathbf{d}$

$$\mathbf{d} \equiv \mathbf{x} - \mathbf{X} \tag{EQ 6}$$

In the analysis of elasto-viscoplastic processes, stresses are attributed only to the elastic part of deformations. For this reason, the elastic part should be isolated from the total deformation gradient. Together with drying effects, the deformation consists of three parts: shrinkage, viscoplastic, and elastic. The deformation gradient can then be represented by multiplication of three components:

$$\mathbf{F} = \mathbf{F}^e \mathbf{F}^{vp} \mathbf{F}^s \tag{EQ 7}$$

where  $\mathbf{F}^e$ ,  $\mathbf{F}^{vp}$ , and  $\mathbf{F}^s$  are the elastic, viscoplastic, and shrinkage deformation gradient respectively. As it happens, this multiplicative decomposition is just an exercise in the chain-rule of differentiation.

Shrinkage is assumed to be isotropic and is given by

$$\mathbf{F}^s = \alpha(c) \mathbf{I} \tag{EQ 8}$$

where  $\alpha(c)$  is the linear shrinkage parameter. For incompressible material,  $\alpha(c)$  can be related to the total volume change as  $(\det \mathbf{F})^{1/3}$ . The volume change, in turn, is governed by the mass transport

equations.  $\mathbf{F}^e$  is calculated as usual and is used to construct the Lagrangian elastic strain tensor  $\mathbf{E}^e$

measured with respect to the stress-free reference configuration

$$\mathbf{E}^e = \frac{1}{2} \left( \mathbf{F}^e \mathbf{F}^e - \mathbf{I} \right) = \frac{1}{2} (\mathbf{C} - \mathbf{I}) \tag{EQ 9}$$

The calculation of  $\mathbf{F}^{vp}$  is taken up below.

### Constitutive Equations

The stress generated by large deformation elasticity for compressible material can be described by:

$$S = \lambda \text{tr}(E)I + 2\mu E^e \quad (\text{EQ 10})$$

where  $\lambda$  and  $\mu$  are Lamé coefficients. Here we write the equation in terms of the second Piola-

Kirchoff stress  $S$ . In any case, this equation is invoked when the "Solid Constitutive Equation" record in GOMA is set to any of the compressible models, viz. not `INCOMP_PSTRESS`, `INCOMP_PSTRAIN`, or `INCOMP_3D`. In contrast, the incompressible form of this equation can be written as

$$S = \pi I + 2\mu E^e \quad (\text{EQ 11})$$

$\mu = \mu(c)$  is the shear-modulus Lamé' coefficient and is in general concentration dependent;  $\pi$  is the pressure associated with incompressibility.  $c$  is the concentration variable which may be present in the model. For the sake of discussion below, we sometimes refer to the deviatoric portion of the

total stress as  $\tau \equiv 2\mu E^e$ . Thus the same deformation can give rise to different stress levels as the solvent concentration changes and the material stiffens. It should be noted that the incompressible form is that which is used with solvent transport to appropriately account for volumetric shrinkage due to solvent transport/loss, as in the saturated-polymer network drying problem of central interest here. It is interesting that in toto, a saturated polymer network is taken as incompressible even though the network itself without solvent may be highly compressible. So it is the transport of the solvent, and the concentration variation without phase change that gives rise to the incompressible nature.

The isotropic term is that which generates the shrinkage stress. The equation for that stress/pressure is the continuity equation:

$$\det(F) = \frac{V}{V_0} \quad (\text{EQ 12})$$

### Viscoplastic Properties

The elasto-viscoplastic model used in this paper does not include work hardening and is based on the yield surface described by the Von Mises condition. For many materials, a Von Mises yield criterion has been found to give results that are good in agreement with experimental data. The yield surface may be a function of several different parameters, including the solvent concentration  $c$ . GOMA currently allows only this dependence, besides the obvious dependence on a yield stress value and the current state of stress. The equation incorporating the effects of solvent concentration on the yield surface can be written in the following general form:

$$\phi(T_s, S_y, c) = 0 \quad (\text{EQ 13})$$

Distributio

Yield stress  $S_y$ , generally a function of the solvent concentration  $c$ , and together with concentration defines the size of the elastic region in the stress space. In the case of coated film, generally no preferred direction is observed in coating material and hence structural isotropy is assumed.

Isotropy, along with the assumption that solvent concentration affects the yield surface only through  $S_y$ , the Von Mises yield criterion can be specified in the following form:

$$\langle \psi(S) - S_y \rangle = \phi \quad (\text{EQ 14})$$

wher  
e

$$\psi(S) = \sqrt{\frac{3}{2} \sum_{klmn} T_{kl} T_{mn} C_{km} C_{ln}} \quad (\text{EQ 15})$$

$$C = F e^T F \quad (\text{EQ 16})$$

and

$$T = S - \frac{1}{3} (S_{ij} C_{ij}) C^{-1} \quad (\text{EQ 17})$$

where  $T_{kl}$  are the components of the deviatoric stress tensor as defined above. With regard to GOMA, we solve Equation 1 in terms of the regular Cauchy stress  $T_s$ , with all transformations to and from the Piola-Kirchoff stress handled within the constitutive equations routines in GOMA. Note that in Eq. 14, we are using as a measure of stress a peculiar invariant of the stress tensor.

The viscoplastic strain rate is assumed to be directly proportional to the excess stress above the yield surface. An associated inelastic flow rule (viz. stress divided by viscosity) is employed here in defining this strain rate. Therefore, the viscoplastic strain rate is expressed as:

$$\tilde{D}^{vp} = \frac{1}{\eta} \langle \psi(S) - S_y \rangle \frac{\partial \psi}{\partial S} \quad (\text{EQ 18})$$

and is applicable only if  $\phi > 0$ .

$\eta = \eta(c)$  is the post-yield viscosity of the material and  $\tilde{D}^{vp}$  is the viscoplastic strain rate, which is the symmetric part of the viscoplastic velocity gradient. This means viscoplastic flow takes place only when  $\phi > 0$  and the flow is faster  $T_s$  is further away from the yield surface. The viscoplastic if deformation gradient is calculated as

$$\tilde{F}^{vp} = \tilde{I} + \int_0^t \tilde{D}^{vp} dt \quad (\text{EQ 19})$$

Note that this integral is readily tracked in an incremental time-dependent calculation because we maintain a Lagrangian mesh, and the history of the strain rate of each material parcel can be associated with each computational entity, or node.

A note for GOMA developers

After introduction of Eq. 9, a deviation from a previous elastic constitutive (developed by Cairncross) has been made. Elastic constitutive equations not employing the EVP formulation are based on an Eulerian formulation. The Eulerian elastic strain tensor  $\tilde{E}$  was calculated as

$$\tilde{E}^e = -\frac{1}{2} \left( \tilde{I} - \left( \tilde{F}^{eT} \right)^{-1} \tilde{F}^{e-1} \right) \quad (\text{EQ 20})$$

This has some ramification on the results below, although no particular advantage is gained by either approach. In summary, when GOMA is used for purely elastic problems and no plasticity equation is invoked, Eq. 20 is used as a strain measure; otherwise Eq. 9 is employed.

For one-dimensional drying problem with close to zero concentration gradient (i.e. very high coating diffusivity) across the coating thickness and a very high yield stress (i.e., one that is not exceeded), the

analytical in-plane tensile stress  $T_s^{xx}$  for the Lagrangian formulation with incompressible elasticity (Eq. 11) is given

by:

$$T_s^{xx} = \alpha^4 \mu \left( \frac{1}{\alpha^6} - 1 \right) \quad (\text{EQ 21})$$

and the analytical pressure  $\pi$  is:

$$\pi = -\alpha^4 \mu \left( \frac{1}{\alpha^6} - 1 \right) \quad (\text{EQ 22})$$

$\alpha(c)$  can be calculated from the displacement at the top of the coating  $d_{top}$  for this particular case with initial coating thickness  $L_0$ :

$$\alpha = \left( \frac{d_{top}}{L_0} \right)^{1/3} \quad (\text{EQ 23})$$

Distributio

However, the analytical in-plane tensile stress  $T^{xx}$  for the Eulerian formulation with incompressible elasticity (Eq. 20) is given by:

$$T_s^{xx} = \alpha^2 \mu \left( \frac{1}{\alpha^6} - 1 \right) \quad (\text{EQ 24})$$

and the analytical pressure  $\pi$  is:

$$\pi = -\alpha^2 \mu \left( \frac{1}{\alpha^6} - 1 \right) \quad (\text{EQ 25})$$

and  $\alpha(c)$  is related the same way to  $d_{top}$  as mentioned above.

With the one-dimensional drying problem laid out above, the analytical solution for plastic yielding with a constant yield stress  $S_y$  and very low plastic viscosity is that  $T^{xx}$  instantaneous turns to  $S_y$  when the coating yields.

We will compare these analytical solutions to those obtained with GOMA in the following section. This memo concludes with some further user/developer notes in the appendix.

## **1D Drying Validation/Test**

Our first test problem and the problem for which this model was developed is that of drying of a gelled polymer film. We consider first the one-dimensional case. The liquid-laden film rests on an impermeable substrate with solvent loss occurring only from the top of the film. The volumetric shrinkage from the solvent loss leads to a rising residual stress during the drying process. Clearly this problem is transient and requires both a momentum balance and a species transport balance. This test problem can be found in the directory `$(GOMA_HOME)/probs/evp/1D_tst`.

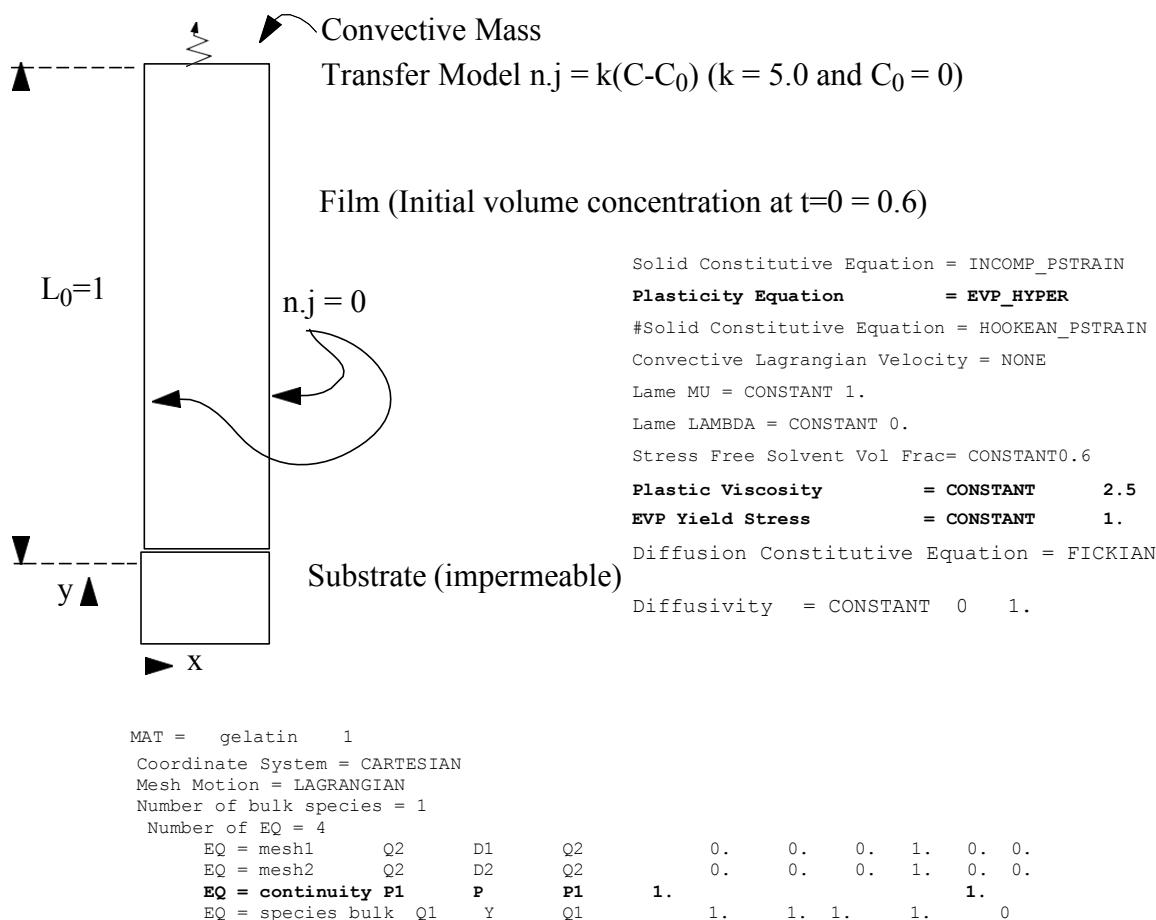
In our sample calculations, we use a stack of five two-dimensional Lagrange finite elements with biquadratic basis functions for the displacements. In this formulation, we take the entire composite of liquid and solid polymer as incompressible, even though the polymer network with the liquid may be compressible. Correspondingly we solve the continuity equation (Eq. 12) together with the momentum equation (Eq. 1) for the pressure and displacement vector. We employ bilinear basis functions for the pressure so as to satisfy the mathematical constraints common when solving equations of this form. Biquadratic basis functions are used to interpolate the concentration of solvent. The initial and boundary conditions of the problem and the relevant thermophysical properties are given in the following figure, together with several relevant portions of the GOMA input file.

The predicted in-plane stress  $T_{xx}$  and free surface displacement for several different cases are shown in the next figure. The properties are kept the same in all cases, with

Distributio

the exception of the yield stress level and the plastic viscosity: we raise the yield stress in one limiting case so as to keep the film deformation purely elastic over the entire drying process. In that way we can compare with the analytical solution given by Equations 21 through 24. In the absence of capillary effects, the total stress normal to the free surface is equal to the ambient pressure, which is taken to be atmospheric so  $T_{yy} = -\pi + \tau_{yy} = 0$  and therefore  $\pi = \tau_{yy}$  everywhere in the film. Because  $\tau_{xx} = \tau_{zz} = 0$  due to problem symmetry, by definition  $\tau_{xx} = \pi$ . The analytical solution for the purely elastic case, or equivalently  $S_y \rightarrow \infty$ , is given by Equation 22.

For the initial conditions used in this test, viz. initial volume fraction solvent of 0.6, the maximum residual in-plane stress according to Eq. 22 is 1.54729. GOMA with the Lagrangian strain measure gives the same, as can be seen in the figure. For a yield stress of 1.0 and a plastic viscosity of 1.0, you can see that the residual stress goes through a maximum value, as expected, after which the film yields and the residual stress drops. For a yield stress of 1.0 and a plastic viscosity of 100, the film stress achieves nearly the same maximum stress as in the purely elastic case, and then drops off more slowly as the film undergoes a slow plastic flow. This recoil-like effect can be expected and gets sharper with falling plastic viscosity.



Distributio

It is interesting to compare the residual stress response of an elastoviscoplastic model such as the one proposed here with a viscoelastic model of the Maxwell variety. Maxwell's stress equation for a viscoelastic material can be written as

$$\frac{d\sigma}{dt} = -E(\sigma/\eta) \tag{EQ 26}$$

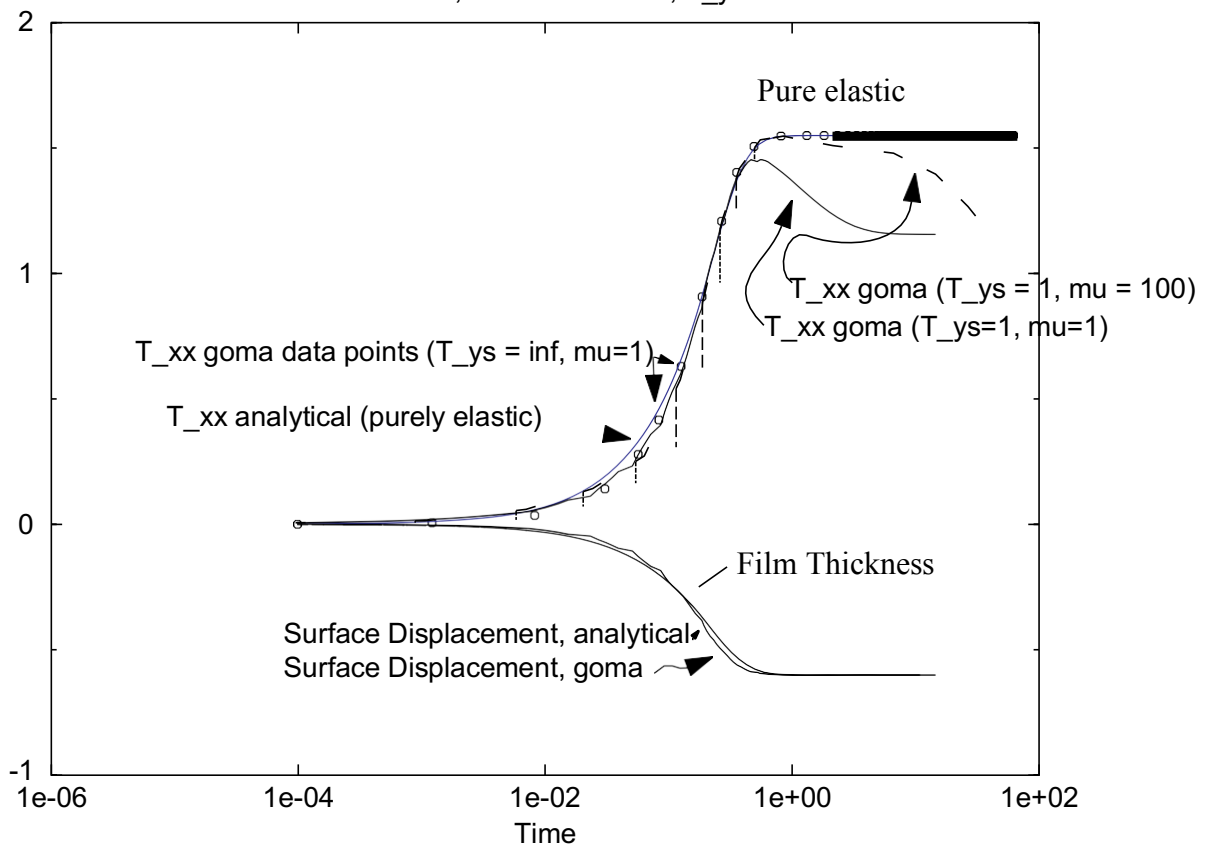
One can integrate this equation from some initial residual stress state  $\sigma_0$  to get

$$\sigma = \sigma_0 e^{-\left(\frac{E-t}{\eta}\right)} \tag{EQ 27}$$

Clearly with this sort of constitutive equation the stress always evolves and relaxes due to the homogeneous nature of the stress rate equation. In other words, materials in this class can not sustain

### 1D Drying Test Case - Analytical Vs. GOMA

Lame Mu = 1, Plastic Mu = 2.5, T\_ys = 1.



a residual stress. Of course you can chose a viscosity so enormous that the relaxation is slow, but strange numerical problems may result.

Christodoulou et al. (1998, "Model of Stress-Induced Defect Formation in Drying Polymer Films", *AIChE J.*, 44, 1484-1498) used versions of this hypoelastic approach to model the same single phase drying problem discussed herein. To derive their version starts with a simple effective stress law in which the solvent stress is taken to be its current pressure, and the polymer, or "contact" stress is derived from first principles using the free energy density of the polymer network. With this they derive a constitutive equation that specializes to the upper-convected Maxwell viscoelastic equation, by invoking a "extra" stress which also satisfies an incremental (differential) law, viz. they really invoke a stress-rate incremental version of a purely elastic solid, with no polymer relaxation. They claim these models can exhibit yielding-like behavior due to their time-dependence but differ from elastic materials in that the stress depends on more than just the current state of deformation, but also the entire deformation path (interestingly though not on the rate in which it is traversed unless a solvent viscosity is added). What is not clear is that in their derivation no viscous term appears explicitly and no stress overshoots are exhibited (we show these below to be related to the rate at which we dry polymer films and associated yield/creep behavior. Christodoulou et al. show that two parameters can be varied to invoke various levels of yielding, rather like we can achieve with the model presented here. Fortunately the EVP model here allows for variation of parameters that are more intuitive in their meaning and invokes no approximation of small deformation. Interestingly, their model yields the same qualitative behavior except that the effect of solvent viscosity is not demonstrated. It is clear that from the EVP model, with high plastic viscosities, we can get yielding without a recoil in stress.

Tam and Lei in their Ph.D. thesis discuss the differences in these two approaches. It is not apparent which one is more advantageous here at this time. The Maxwell model above can lead to similar stress profiles in the elastic limit, but effectively such materials are continuously flowing/yielding under any stress. The EVP model will support a stress without yielding, so long as the stress does not exceed a critical value. It seems as though many solidified coatings behave in this fashion.

## **2D Drying/Validation with Gelatin Beam Bending Apparatus**

This test problem can be found in [\\$\(PROBS\)/evp/evp\\_probs/beam\\_evp](#). Basically it is set up as close as possible to simulate the conditions of the drying of a gelatin material as described in detail by Lu, et. al. (2000): *CRMPC Report on Gelation: Probing Plastic Deformation in Gelating Film During Drying*, by M. Lu, S. Y. Tam, A. Sun, P. R. Schunk and C. J. Brinker. This report can be obtained from the CRMPC contacts at Sandia. Basically the experiment involves a cantilever beam apparatus built inside of an environmental control chamber. A strip of double sided-polished silicon wafer (dimensions below) is coated on one side with the test material (photographic-grade gelatin in this case), and clamped at one end in the apparatus. A He-Ne laser is used to detect the free end deflection by measuring the displacement of the laser spot that bounces off the beam free end using a photo-sensitive detector. The in-plane stress of the film is then calculated by Stoney's equation, which is derived from linear elasticity:

Distributio

$$\sigma_{xx} = \frac{E_s d_s^2}{3L^2(1 - \nu_s)d_f} \delta \quad (\text{EQ 28})$$

Here  $E_s$  - Young's modulus of silicon -  $1.48 \times 10^5 \text{ MPa}$ ,  $d_s$  - Substrate thickness -  $75 \mu\text{m}$  or  $150 \mu\text{m}$ ,  $L$  - Substrate length,  $\nu_s$  - Poisson's ratio of silicon -  $0.18$ ,  $d_f$  - film thickness, and  $d$  - free end deflection measured.

Other relevant conditions in the simulation are (see **Defs** file in test directory):

```
$ {init = 0.5} (Initial volume fraction water)
${keff= 100.} micron/sec (Mass transfer coefficient, which is varied from 1 to 100)
${h_ref = 10} micron (reference length and initial film thickness)
${width = 50000/h_ref} micron/micron
${h_silicon = 150/h_ref} micron/micron
${h_gel = 10/h_ref} micron/micron
```

```
$Properties of silicon
${mw_sil = 28.0855} gm/gm-mol
${rho_sil = 2.33} gm/cc
${cp_sil = 4.78/mw_sil} cal/gm-K
${k_sil = 0.353} cal/sec-cm-K
${lame_ref = 35275e+06*10.} dynes/cm2
${lame_mu = 35275e+06*10/lame_ref}
${lame_lambda = 62712e+06*10/lame_ref}
```

```
$Properties of gelatin
$ use water for now
${rho_gel = 0.8} gm/cc
${cp_gel = 1.} cal/gm-K
${k_gel = 5.92*0.860421} cal/hr-cm-K
${k_gel = k_gel/3600.} cal/sec-cm-K
${mu_gel = 0.8904*.01} gm/cm/sec
${d_gel = 2.e-9*1.e6*1.e6} micron2/sec
${lame_mu_gel = 1000/lame_ref}
${lame_lambda_gel = 1.e3/lame_ref}
```

```
$Initial conditions
${Xinf = 0.3} (Relative Humidity of surrounding air)
${inv_charac_time = d_gel/h_ref/h_ref}
${diffu_gel = d_gel/d_gel}
${keff_gel = h_ref*keff/d_gel}
```

The conditions for the experiments of Lu, et al. (2000) differed from these simulations mainly in the following way:

- Initial film thickness from 1 to 2 microns (as opposed to 10 microns here)
- Relative humidity is held fixed here at 30 percent and the calculation is isothermal, for now.
- The diffusivity, gel elastic moduli, yield stress, and plastic viscosity were all held constant

It is also noteworthy that we approximated the mass transfer coefficient (which we vary below), the diffusivity and the film thickness, which for computational convenience in meshing aspect ratios we

take as 10 microns, whereas all the experiments are performed with initial gelled thickness of less than 2 microns (cf. with experiments of J. Payne (1998 Ph. D. Thesis, University of Minnesota)).

The results are plotted up in the included figure. We show the mesh/geometry, which due to the large aspect ratios turns out to be poorly resolved, and a zoom of the mesh/geometry at the end of the beam after a significant amount of drying. Noteworthy is the shrinkage effect on the end of the film which produces local high stress, but relatively low integrated force on the beam. Accompanying the mesh/geometry figures is a plot of the in-plane stress vs distance along the substrate (upper x-y plot), at the substrate/film interface, and the in-plane stress as a function of time at one point in the film for several different conditions (lower x-y plot).

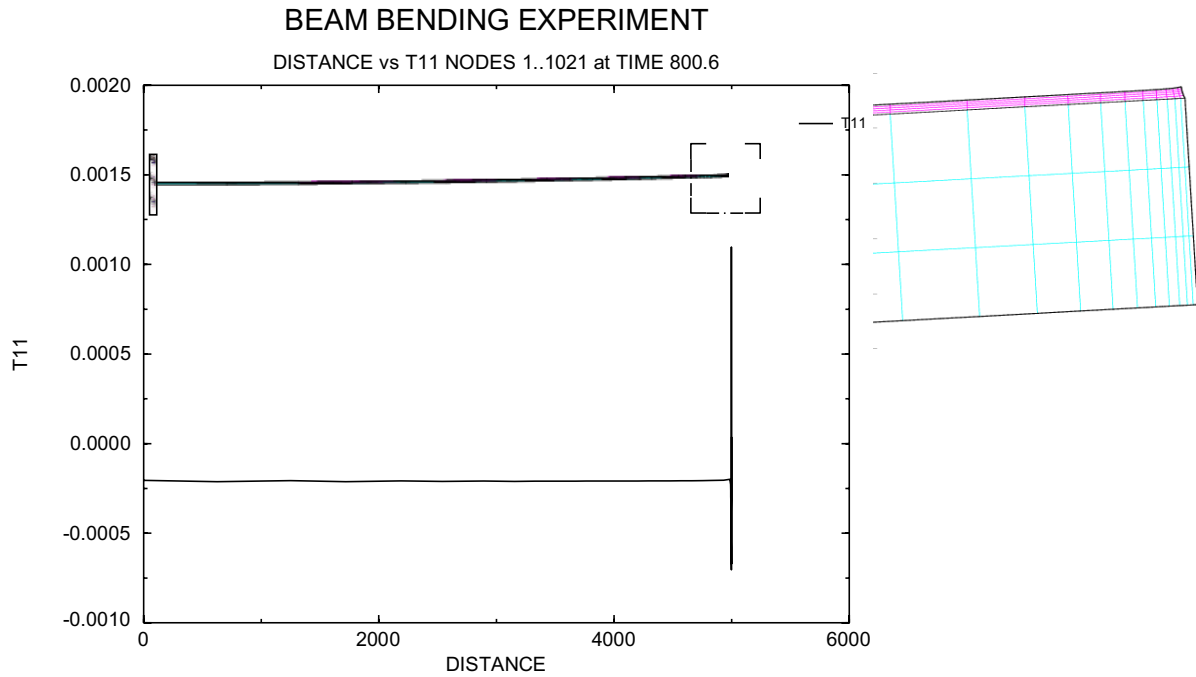
From the stress profile it is clear that the solution is clearly zero-dimensional and only a function of time, viz. no variation in the stress can be seen along the length of the substrate, except the singular like behavior at the edge. The implication of this is that when the film yields, it yields along the entire length of the film at the same time--although it yields at the edge at a much earlier time the effect on the deflection is negligible.

In the time-history plots we examine the in-plane stress at several different conditions. Specifically we vary the yield stress in the range of 300 MPa to 0.03 MPa and a drying rate from 1 micron/s to 100 micron/s. Altogether stress profiles for seven parameter sets are shown. We will now compare these results qualitatively to those of Lu, et. al. (2000).

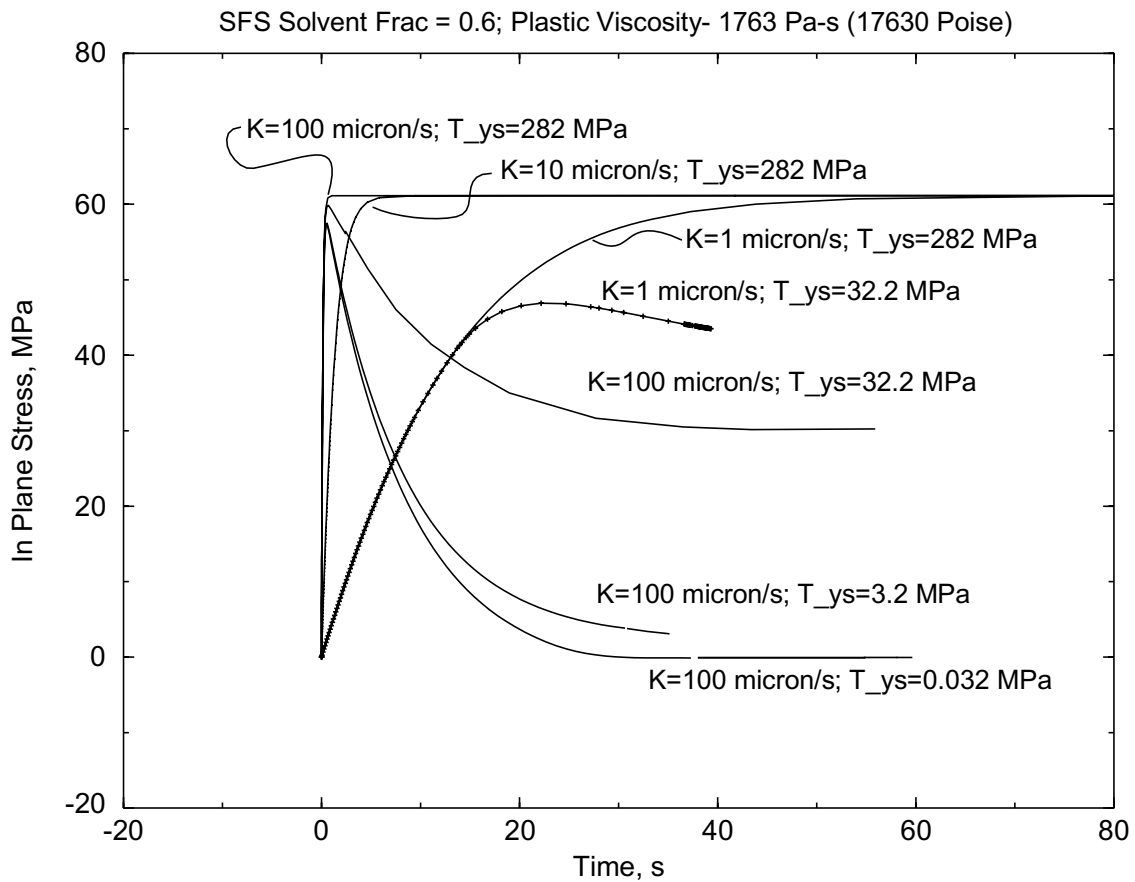
As for the stress levels we are predicting very close to the residual stresses measured with Stoney's equation and the cantilever beam apparatus. Note that we predict a maximum stress of the order of 65 MPa. Although Lu, et al. never ran these exact conditions, similar drying extents and drying rates produce the same order of stress. We also predict very similar free-end deflections (of the order of 1 to 2 mm). For our test cases we would expect higher deflections than in the experiments if the drying extent and rate were matched because of the thicker film we use, assuming the film never yields.

Most encouraging is that we are predicting all of the fundamental trends that are seen in the experiments. First, with a yield stress of 282 MPa, the film never yields and you get the familiar purely elastic response (see 1D test above) with no stress overshoot. In the experiments the films always yielded, but then again they did not have the luxury of changing the yield stress. If we lower the yield stress to 35 MPa, we see yielding in our numerical tests, as is indicated by the stress overshoot and then a relaxation to a lower residual stress. This is exactly the behavior observed by Lu, et al., even on similar time scales. Most encouraging is that we can influence the final residual stress by the rate of drying, which was one of Lu et al.'s experimental findings. And, his measured plastic yield stress is the one we used to achieve a yielding behavior.

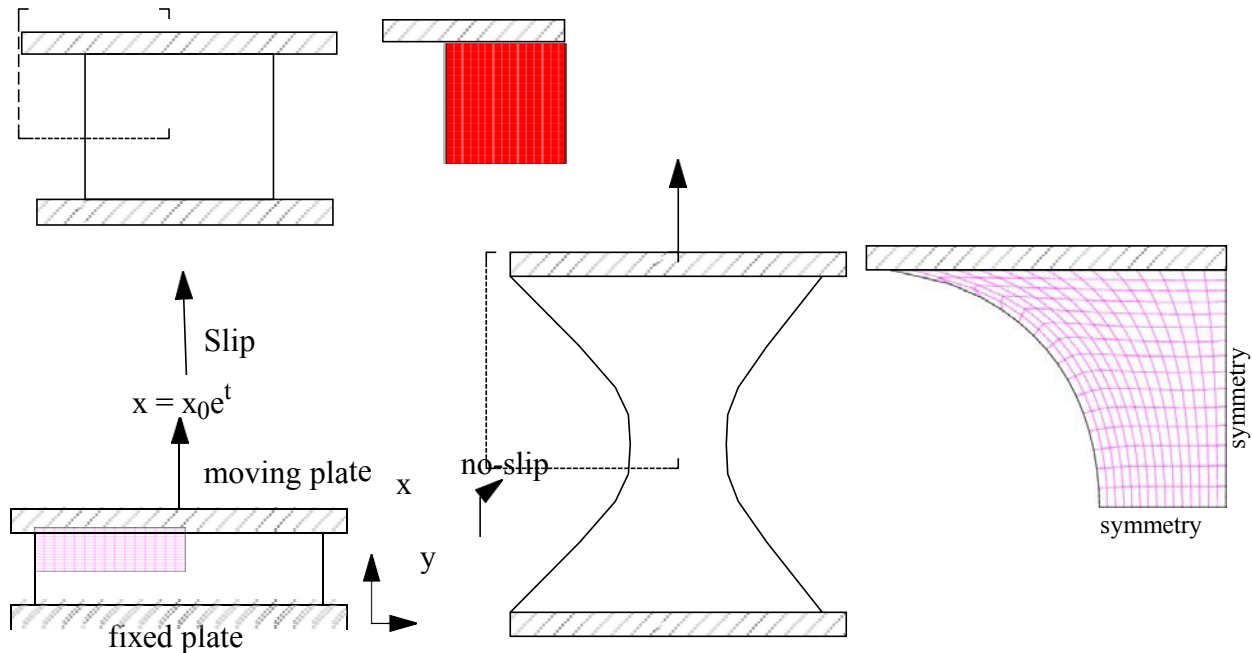
All told, it appears the GOMA model and the EVP constitutive equation allows us to predict all of the features and the trends seen in the experiments, suggesting further work into using GOMA to perform parameter estimation on a variety of systems to determine characteristic yield stresses and plastic viscosities. We think this is achievable under the right conditions so long as they are managed to keep gradients in solvent concentration out of the film, thereby reducing the sensitivity to the sometimes



### Beam Bending - Gelatin films



Distributio



immeasurable diffusivity and provided we can model thinner films (of the order of 2 microns).

Moreover, these calculations still need to be repeated with variable thermophysical properties (temperature and volume-fraction solid/liquid effects on the elastic constants and transport properties).

### Filament/Sheet Stretching

Our third test problem is one which has nothing to do with drying or solvent transport, but instead allows us to explore the effect of imposed deformations on the elastic stress together with subsequent yielding and plastic flow of a simple test piece. We examine a simple planar/2D test piece and subject it to unidirectional (not uniaxial since this is not an axisymmetric problem) deformation, viz. this is a plane strain problem.

Furthermore, so we can compare it with some other test problems we are running with Newtonian fluids and with viscoelastic fluids, we run this problem in a sheet stretching mode, as diagrammed below. Right now the EVP constitutive equations are limited to plane-strain problems so we cannot run the axisymmetric case. The problem itself can be found in  $\$(PROBS)/crmpc\_filament$ . In there you will find two input decks: **filament.inp** and **filament\_solid.inp**. The first corresponds to a purely inelastic material and is an ALE calculation of an incompressible flow. The second input deck corresponds to a elastic or elastoviscoplastic material, and the problem is of course set up as purely Lagrangian.

Our goal here is to test the behavior of a EVP material under several different yield stresses and plastic viscosities, while undergoing a time-dependent strain as diagrammed above. The time-exponential

Distributio

increasing strain was chosen such that the Hencky strain increases linearly with time, the Hencky strain being defined as  $\ln(x/x_0)$ . The problem description figure above shows that we run two different sets of boundary conditions on the moving and fixed plates (actually, we do not extend the model to the fixed plate as we take advantage of two symmetry planes, as shown). In the first case we assume a no-slip condition, i.e., perfect adherence, of the test material on the moving plate. This corresponds to setting the y-displacement along the plate to zero. In the second case we allow perfect slip in the lateral, y-direction, which is accomplished simply by not constraining the y-directed displacement. The reason we ran this latter case is that we find the singular stress at the contact line (upper left of the figure) leads to excessive yielding and large plastic flow. This greatly distorts the mesh at early times, as shown in the figure. Although you can restart the calculation after remeshing (discussed below), this is tedious.

It should be pointed out that we are not running this calculation with an incompressible material model. We have recently refurbished the EVP constitutive equation so that one can run the compressible case (viz. Eqn 10). To invoke this version we used the INCOMP\_PSTRAIN model for the Solid Constitutive Equation. Notice that in that model the compressibility is measured by the entire deformation, as the trace of the strain tensor  $E$  is used as a measure of volume change. It is not clear what the numerical ramifications are for doing this is, as plastic flow that is compressible may lead to pressure singularities.

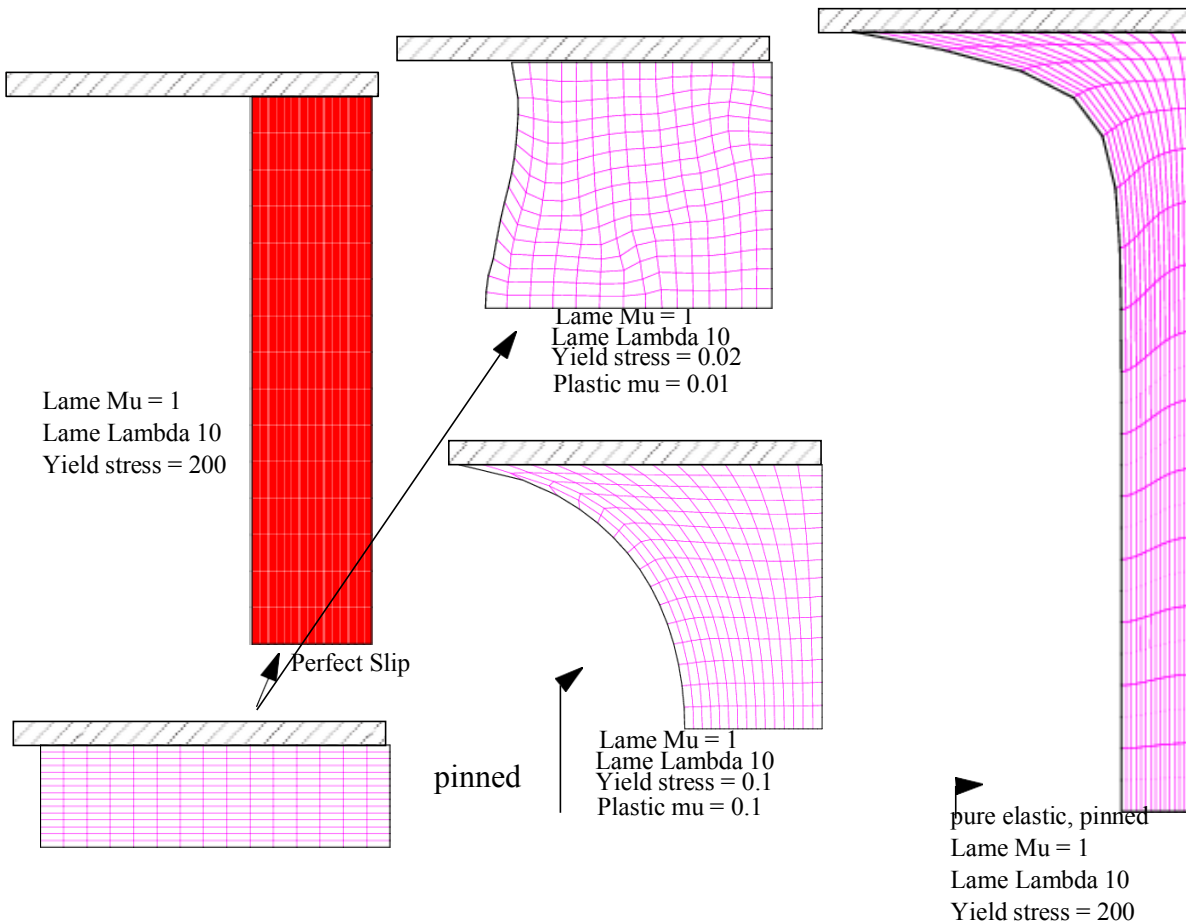
Some sample results are shown in the figure above. We show two tests for the pinned, no-slip case (results to the right). The purely elastic case (furthest right) runs easily to large strains despite the large stress that develop. The scale is held constant from the initial to the final case, clearly indicating that the sample is expanding as it is being stretched. If we lower the yield stress from 200 down to 0.1, we find that the calculation stagnates at a much small strain. Close examination of the mesh shows that plastic flow is occurring along the free surface and in the contact line region. This plastic flow greatly distorts the mesh and the calculation stops. We were able to restart the calculation with a new mesh but quickly found a singular behavior.

For the perfect slip case we were able to achieve much higher strains for yielding materials. The figure shows however one case in which we impose a very low yield stress (0.01) and a low plastic viscosity (0.01) which leads to rapid thinning and an unstable incipient necking failure mode. The calculation could not be restarted even after a remapping step.

The final figure below shows the integrated axial stress on the moving plate for three different cases. The purely elastic case was invoked by setting the yield stress to be a large value. You notice that the force on the moving plate increases monotonically as the strain increases. A second case corresponds to a low yield stress (unity). When the work piece stress exceeds the yield stress at a strain of about 0.5, the force on the plate begins to decrease with continued strain, indicating plastic flow with a small viscosity. If instead the viscosity is raised to 10 (from 0.1) and the yield stress is decreased further to 0.01, the force falls off the elastic limit at much small strains, as expected, but does not decrease with strain due to the action of viscosity. All of these behaviors seem intuitive.

Further testing of this mode of usage is still needed. Perhaps the biggest need is to extend the formulation to axisymmetric and to three-dimensional geometries.

Distributio

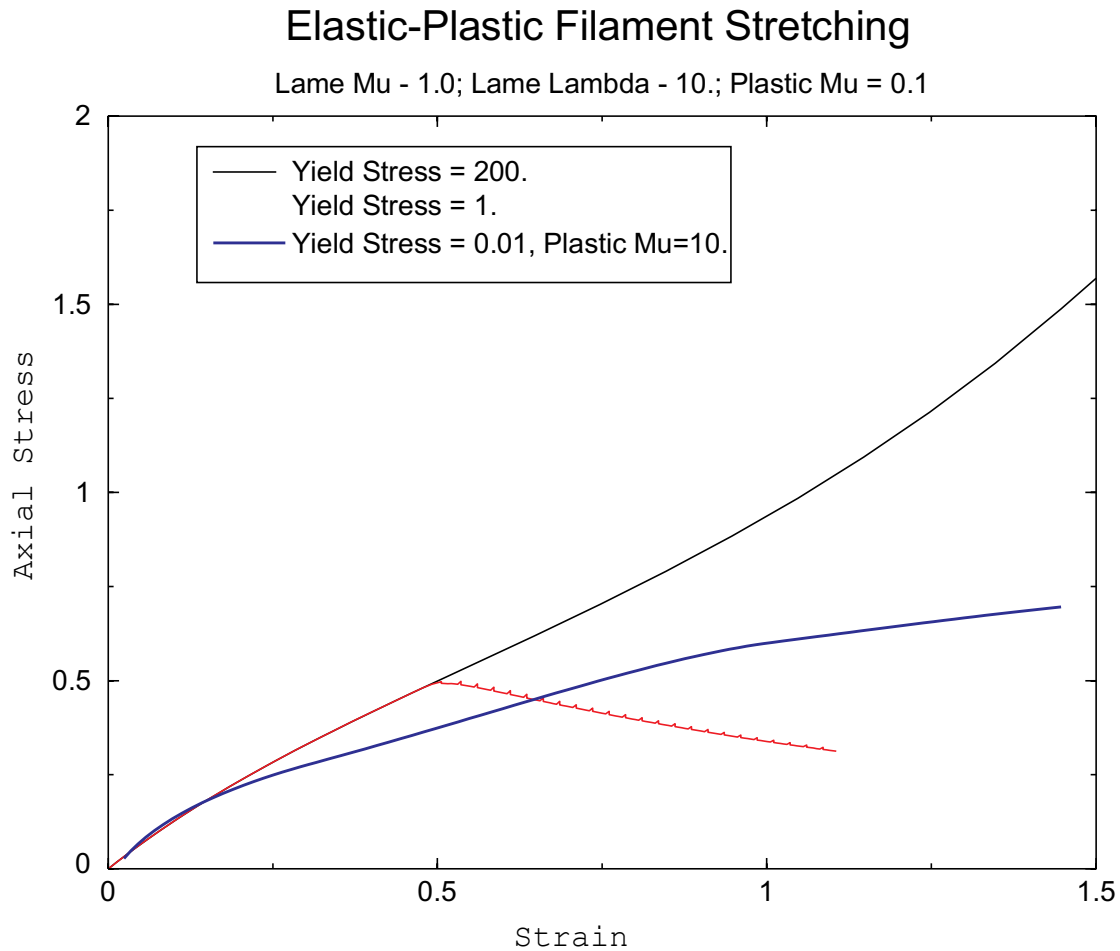


## User's Guide

This user's guide assumes the user has used GOMA to solve elastic problems due to drying before. Therefore the discussion only addresses the additions and differences between the elastic case and elasto-viscoplastic case.

### Material File

There are several new cards added to the material file, namely, **Plasticity Equation**, **Plastic Viscosity**, and **EVP Yield Stress**. To evoke the elasto-viscoplastic constitutive model, one should enter **EVP\_HYPER** in the **Plasticity Equation** card in the material file. Also, the **Plastic Viscosity** and **EVP Yield Stress** cards should be entered. There are two model options for both the **Plastic Viscosity** and **EVP Yield Stress**, **CONSTANT** and **LINEAR**. If a **CONSTANT** model is chosen for any of these quantities, then only one real number is entered following the model name. If a **LINEAR** model is chosen for any of these quantities, then two real numbers are entered following the model name. *NOTE: this model activates a linear dependence on concentration and hence can only be used for cases in which there is solvent transport.* For other dependencies this model will have to be



furnished. The two real numbers can be entered in any order. GOMA automatically sets the smaller number to be the initial value at solidification. The quantities increase linearly as the decrease in solvent concentration during drying. The larger number is the ultimate value when the coating is complete dried. Given two real numbers in ascending order  $y_1$  and  $y_2$  the quantity at a certain concentration  $c$  is:

$$y = y_1 + \left( \frac{V_{sf} - c}{V_{sf}} \right) (y_2 - y_1) \tag{EQ 29}$$

## Distributio

where  $V_{sf}$  is the stress free solvent volume and the solvent volume at solidification, which is set with the **Stress Free Solvent Vol Frac** card in the material file. In summary for a drying/ solidification problem, the material file input deck requirements are shown as follows:

```
Stress Free Solvent Vol Frac   = CONSTANT   0.6
Plasticity Equation            = EVP_HYPER
Plastic Viscosity              = LINEAR       1.0   2.0
Evp Yield Stress               = CONSTANT   50.0
```

There is one new model added to the Lamé coefficient  $\mu$ . The model for Lamé coefficient  $\mu$  with the input record name **Lamé MU** can be chosen as **CONSTANT** or **DENSE\_POWER\_LAW**. Note that there are other possible input model names for the card **Lame MU** but they are only relevant to other applications. If model **CONSTANT** is chosen for this card, then only one real number is entered after the model name. If model **DENSE\_POWER\_LAW** is chosen for the card, then two real numbers are needed after the model name. The first real number is  $\mu_0$  and the second real number is the power

$n$ .  $\mu$  rises from zero at solidification and reaches  $\mu_0$  as the coating dries. The higher the power  $n$ , the more delay in stress development but with a steeper rise in stress values later on. This model is designed to describe stress development in gelatin coatings. The formula is:

$$\mu = \mu_0 \left[ \frac{1 - \det | \cdot |}{1 - V_{sf}} \right]^n \quad (\text{EQ 30})$$

The input deck requirement in the material file for this model is:

```
Lame MU   = DENSE_POWER_LAW   100.0   4.5
```

For incompressible elasto-viscoplastic material, Lamé coefficient  $\lambda$  is not used and the value of  $\lambda$  will not enter into calculation.

*Incompressible, Yielding Elastic/Plastic solids with No Species Transport*

It should be noted that the EVP model has been furnished to run problems of basic elastic/plastic deformation for incompressible and compressible materials. Some usage tips here are noteworthy. If one desires to study the deformation of an *incompressible* solid material that is characterized by elastic constants, yield stress, and a plastic viscosity, but contains no transport of solvent, then the species transport should be turned off in the GOMA input file, the continuity equation should be turned on with both multipliers (viz. Eq. 12 with the right hand side equal to unity), e.g.

MAT = coating 1

Coordinate System = CARTESIAN

Element Mapping = isoparametric

Mesh Motion = LAGRANGIAN

Number of bulk species = 0

Number of EQ = 3

## Distributio

```

EQ = mesh1      Q2  D1 Q2      0.  0. 0. 1. 0.
EQ = mesh2      Q2  D2 Q2      0.  0. 0. 1. 0.
EQ = continuity P1  P   P1      1.                1.
                div ms adv bnd dif src por

```

together with the following settings in the material file `coating.mat`:

```

Solid Constitutive Equation = INCOMP_PSTRAIN
Plasticity Equation        = EVP_HYPER
#Solid Constitutive Equation = HOOKEAN_PSTRAIN
Convective Lagrangian Velocity= NONE
Lame MU                    = CONSTANT      1.
Lame LAMBDA                = CONSTANT      0.
Stress Free Solvent Vol Frac = CONSTANT    0.0
Plastic Viscosity          = CONSTANT      2.5
EVP Yield Stress           = CONSTANT      1.
$EVP Yield Stress          = CONSTANT      0.1

```

Note that the stress free solvent volume fraction is set to zero, which is necessary to achieve unity on the right-hand-side of Eq. 12.

Compressible, Yielding Elastic/Plastic solids with No Species Transport

Sometimes one just wants to study the deformation of a general compressible elastic solid with a yield-point and which undergoes plastic flow above that point. GOMA has been furnished to run in this mode as well, which can be invoked again by shutting off species transport as described above, turning off the continuity equation, as it is no longer needed for a compressible material, and selecting one of the compressible elastic formulations for the Solid Constitutive Equation in the material file. As an example:

```

MAT = coating 1

Coordinate System = CARTESIAN
Element Mapping = isoparametric
Mesh Motion = LAGRANGIAN
Number of bulk species = 0

Number of EQ = 2
EQ = mesh1      Q2  D1 Q2      0.  0. 0. 1. 0.
EQ = mesh2      Q2  D2 Q2      0.  0. 0. 1. 0.
                div ms adv bnd dif src por

```

together with

```

Solid Constitutive Equation = HOOKEAN_PSTRAIN
Plasticity Equation        = EVP_HYPER
#Solid Constitutive Equation = HOOKEAN_PSTRAIN
Convective Lagrangian Velocity= NONE
Lame MU                    = CONSTANT      1.

```

## Distributio

Lame LAMBDA	= CONSTANT	0.
<b>Stress Free Solvent Vol Frac</b>	<b>= CONSTANT</b>	<b>0.0</b>
Plastic Viscosity	= CONSTANT	2.5
EVP Yield Stress	= CONSTANT	1.

Note that the solid constitutive equation in this case is set to an elastic plain strain model of the NeoHookean variety.

Input File

There is one new output parameter card added to the input file: Viscoplastic Def\_Grad Tensor. This card output the quantity  $\mathbf{F}^{VP}$ . If the material is still in the elastic regime, the  $\mathbf{F}^{VP}$  is an identity tensor/ matrix. Once the material starts to yield, this quantity starts to depart from the identity matrix. The entry in the input file is:

```
Viscoplastic Def_Grad Tensor= yes
```

If you also turn on the **Mesh Stress Tensor** post processing option, you will get the components of the viscoplastic stress tensor (as **TVP11**, **TVP12**, etc. in the ExodusII file) as well as the total stress  $T_s$  (as **T11**, **T12**, etc. in the ExodusII file). These stresses are nodal variables. In fact you need both the **Viscoplastic Def\_Grad Tensor** record and the **Mesh Stress Tensor** record set to “yes” in the input deck to do a restart (see below).

Restarts

Restarting an EVP problem becomes necessary due to mesh distortion or premature termination of a transient run. Sometimes you would like to change the conditions of a problem from its current state and then continue the calculation. Restarting these problems requires more information than what is typically read in from a solution in the standard ExodusII file, if the material has already yielded. Due to the fact that we need the viscoplastic strain tensor components for a restart, and that these components are not primitive variables, we need to read these components and the viscoplastic stress tensor components from the restart ExodusII file for a smooth restart. A quick examination of Eq. 19 and its dependencies on the viscoplastic stress hints to these need. We have upgraded GOMA recently to allow restarts, but in somewhat of an unorthodox way. Because GOMA restarts from exoII files intrinsically means that restarts are from primitive variables only, a simple `read_exoII` or `read_exoII_file` option will not pick up these tensor components. To get them you first must make sure they exist in the restart file. This will be the case if you activate the printing of these tensor components in the output Exodus II file as explained above. You can then use the external variable capability (cf. GM-03.3 for a complete explanation) to activate a smooth restart. Notice in the input deck fragment below how we read from the `restart_exoII` file first, to get the primitive variables, and then read from it again with the added external variable cards to get each of the components.

Another side note: notice how we no longer initialize the mass fraction of the liquid in the solid (commented out), as the concentration will be read from the restart file.

A final note: if your material has not yet yielded, than you can restart from just the primitive variables as usual, as the viscoplastic strain and stress tensor components are known.

Distributio

```

$Initial Guess = zero
$Initialize Mass Fraction = 0.5
Initial Guess = read_exoII_file restart.exoII
External Field = FVP11 Q1 restart.exoII
External Field = FVP22 Q1 restart.exoII
External Field = FVP33 Q1 restart.exoII
External Field = FVP12 Q1 restart.exoII
External Field = FVP21 Q1 restart.exoII
External Field = TVP11 Q1 restart.exoII
External Field = TVP22 Q1 restart.exoII
External Field = TVP33 Q1 restart.exoII
External Field = TVP12 Q1 restart.exoII
External Field = TVP21 Q1 restart.exoII

```

### **Problem Shooting – running the drying problem and EVP**

*Problem* – Trouble in continuing the first few time steps.

*Solution* – You may have a fast drying case with slow diffusion in the coating. Instead of decreasing the time step size according to the normal procedure and intuition, *increase* the time step size. With fast drying and slow diffusion, the initial concentration gradient is very steep at the drying surface. This is a very difficult numerical problem to solve. So when you increase the time step size, in effect, you are relaxing the concentration gradient the program is solving, that will get you pass the initial numerical difficulty. However, even if the code can handle such condition, the concentration and stress profile may appear very wavy. This waviness only reflects the degree of difficulty the code encountered and is not part of the real solution. In this case, refining the mesh towards the drying surface will only increase the waviness of the solution. Drawing from this observation, *coarsening* the mesh will also get you pass this initial numerical difficulty. Although this condition may post numerical stability problem initially, it does not affect subsequent solution. And most of the time, one is not interested in solution of initial time steps.

*Problem* – Trouble in converging in the plastic region.

*Solution* – Reduce the time step size because viscoplasticity is in itself a time dependent problem and elasticity in itself is not. Before the material yields, time dependency is induced only through the drying process. The reduction in time step size depends on the value of the plastic viscosity. The lower the viscosity, the small time step should be used. Also, it takes more iterations to converge a time step in the viscoplastic region than the elastic region, so increasing the maximum allowable iterations per time step will help.

#### Other Cautions:

Always set the MASS\_FRACTION in the input file to be the same as the Stress Free Solvent Vol Frac in the material file.

The code has been tested for a wide range of initial solvent volume (up to 0.85). When using very high initial solvent volume (approaching 0.85 or beyond), use with caution.

Distributio

Notes on development and trouble shooting:

Developer: evpl-> is viscoplasticity  
structure

Developer: Notice that this evpl struct is not in  
dp\_vif.f Developer and user: Set up for plane strain  
only just now

Developer: get\_evp\_stress gets its own elastic contribution and does not use what is  
computed in mesh\_stress\_tensor

Developer: Need really to reorganize how the elastic stress is computed in all cases EVP  
or not in mesh\_stress\_tensor. There are some redundancies in there for the isotropic  
term.

Test problem dirs: `evp/1D_tst`, `crmpc_filament`, `evp/evp_probs/beam_evp`

Notes on Post processing:

TT from mesh stress tensor are the total stresses, with pressure/volumetric term. tvp11  
etc. are just the deviatoric part.

To run compressible with lame coefficient:

Solid Constitutive Equation = `NONLINEAR, HOOKEAN_PSTRAIN`

To run incompressible without concentration equation:

Solid Constitutive Equation = `INCOMP_PSTRAIN, INCOMP_PSTRESS`

and set continuity equation on with all 1s to turn on all terms. And set Solvent fraction of  
SFS to zero

Still to do:

TALE, Porous, etc. with this model